Chemistry Research Journal, 2018, 3(6):49-57

Available online www.chemrj.org

Research Article

ISSN: 2455-8990
CODEN(USA): CRJHA5

Theoretical study of relation between electronic structure and antiplasmodial activity of chalcone derivatives

Wilfried Anatovi, Gaston A. Kpotin, M. T. Alice Houngue Kpota,Urbain A. Kuevi, Guy S. Atohoun, Jean-Baptiste Mensah

Laboratory of Theoretical Chemistry and Molecular Spectroscopy (LACTHESMO), Faculty of Sciences and Techniques (FAST), University of Abomey–Calavi(UAC);03 BP 3409 Cotonou, Benin

Abstract Malaria is a parasitic disease that is widespread in the world and endemic to intertropical zones. According to World Health Organization, Africa is the most affected by malaria, especially in its sub-Saharan zone. Important work has been done on malaria, however, there are some drug resistance developed by certain strains of *plasmodium.* This work aim to propose a model of antimalarial 2D-pharmacophore based on a theoretical study of the relation between the electronic structure of a series of molecules derived from chalcone and the antiplasmodial activity in vitro against the *pf*3D7 strain. This QSAR study was done according to the Klopman-Peradejordi-Gòmez technique (KPG). Using the Gaussian program, the DFT / B3LYP method in the 6-31G database (d, p), the optimization of the geometries of the molecules was done. After a multiple linear regression using Statistica software, an equation expressing log (IC_{50}) as a function of eight molecular reactivity indices was obtained. Analysis of the results made it possible to propose a 2D pharmacophore; this will enable us to propose more reactive antimalarial molecules. The process seems to be charge and orbital-controlled.

Keywords Chalcone; antimalarial activity; pf3D7 strain; QSAR, DFT, KPG approach

1. Introduction

Malaria is currently recognized as one of the intercontinental tropical infectious diseases that affects our populations [1]. With more or less different clinical effects, malaria is caused by parasites of the genus *Plasmodium* [2]. Although four *Plasmodium* species (*P. falciparum*, *P. vivax*, P. *ovale*, and *P. malariae*) cause human malaria, *Plasmodiumfalciparum* is the most virulent.The infections caused by *Plasmodium falciparum* is prevalent in the major parts of Africa, sub-Saharan Africa and East Asian countries [3], whose strain *pf*3D7 [4] was the subject of our study. Parasites are transmitted to humans by the bite of a vector; it is the infested Anopheles female mosquito, which usually stings in the early evening and in the deep night [5]. Through its saliva which plays a sedative role during its blood meal, the infested female Anopheles ingests in the blood of a receptive subject; parasites of the genus *Plasmodium*pursue part of their cycle evolutionary in human blood [1]. These parasites haematozoa developing and subsequently trigger various clinical effects of malaria (high fever, migraines, chills and anemia) [6]. In the light of the different antimalarial treatments against malaria [7-9], there are also some plasmodial strains that develop bio-resistant factors and become more and more chemo-resistant [10-12]. Various malaria vaccines are in the experimental phase [13-15]. A large list of drugs such as Quinine, Primaquine, chloroquine, mefloquine, halofantrine, lumefantrine, piperaquine, proguanil and artemisinin derivatives (artemether, artemminol, dihydroartemisinproguanil) [4] are used to treat malaria. But each of these drugs has one or more problems such as

inefficiency or is a source of toxicity or resistance during treatments of malaria phases. Previous work has shown that chalcone compounds have interesting antibacterial, antileishmanial [16-19] and especially antiplasmodial properties, [20-24]. These properties are expressed through the IC_{50} values of each molecule. By the theoretical chemistry combined with the Quantitative Strutural Analysis Relationship (QSAR) [25-26] we present a study of the relationship between the electronic structure and the antiplasmodial activity of chalcones on malaria.

2. Methods, materials and calculations

2.1 Method and material

The method used to determine the quantitative relationship between structure-activity is the Klopman-Peradejordi-Gómez (KPG) method. This methodology used here to find the relation between the electronic structure and the inhibition constant is widely discussed and applied in several works, we present a summary below [27-30]. The median inhibition constant IC_{50} can be expressed as a linear relation of the form:

$$\log(IC_{50}) = a + \sum_j \left[e_j Q_j + f_j S_j^E + s_j S_j^N\right] + \sum_j \sum_m \left[h_j(m) F_j(m) + x_j(m) S_j^E(m)\right]$$

$$+ \sum_j \sum_{m'} \left[r_j(m') F_j(m') + t_j(m') S_j^N(m')\right] + \sum_j \left[g_j \mu_j + k_j \eta_j + o_j \omega_j + z_j \varsigma_j + w_j Q_j^{\max}\right] + \sum_{k=1}^{U} O_k \qquad (1)$$

S_j^E and S_j^N are, respectively, the total atomic electrophilic and nucleophilic superdelocalizabilities of atom j.

$F_{j,m}(F_{j,m'})$ is the Fukui index of the occupied (vacant) MO m(m') located on atom j [31]

$S_j^E(m)$ is the atomic electrophilic superdelocalizability of MO m on atom j,

$S_j^N(m)$ is the atomic nucleophilicsuperdelocalizability of MO m' on atom j

The total atomic electrophilic superdelocalizability of atom j corresponds to the sum over occupied MOs of the $S_j^E(m)$'s and the total atomic nucleophilicsuperdelocalizability of atom j is the sum over vacant MOs of $S_j^N(m)$'s[27].

μ_j is the local atomic electronic chemical potential of atom j, η_j is the local atomic hardness of atom j,

ω_j is the local atomic electrophilicity of atom j,

ς_j is the local atomic softness of atom j, and

$Q_j^{\max}$ is the maximum amount of electronic charge that atom j may accept from another site [27]

O_k 's are the orientational parameters of the substituents[32].

Throughout this paper $HOMO_j^*$ refers to the highest occupied molecular orbital localized on atom j and $LUMO_j^*$ to the lowest empty MO localized on atom j. They are called the local atomic frontier MOs.

The application of this method (equation (1)) has yielded exceptional results for a large number of systems diversity: Drug-Receptor in several studies [33-38].

For the application of this method, a series of twenty-four molecules [39] are selected from chalcone derivatives whose basic structure is the main compound is (E) 1,3-diparaphenylprop-2-en-1 one, whose experimental antiplasmodial activities are known. The structures of these compounds are summarized in the model of Figure 1 below. Table 1 summarizes the values of the experimental median inhibitory concentrations of each molecule: these values come from the literature [39]. These tests were performed on the blood form of plasmodium *pf*3D7 strain.

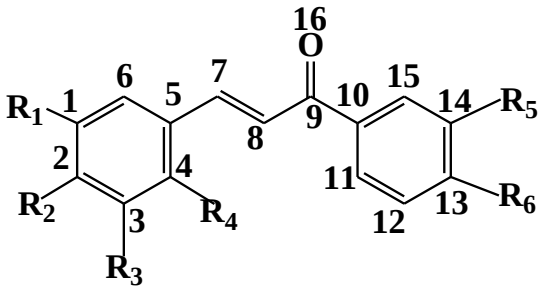

Figure1: General structure of the 24 Chalcones derivatives

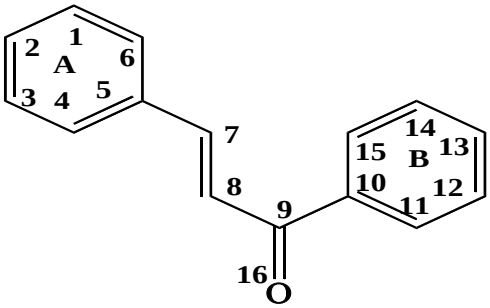

Figure 2: Common skeleton of studied chalcones

Table I: Structures of chalcones studied.

Molecules	R1	R2	R3	R4	R5	R6	log(IC_{50})
1	Allyl	OH	OCH_3	H	H	4-OH	1,585
2	Allyl	OH	OCH_3	H	H	4-Cl	1,447
3	Allyl	OCH_3	OCH_3	H	H	4-Cl	0,591
4	Allyl	OCH_3	OCH_3	H	H	4-OCH_3	0,633
5	Allyl	OCH_3	OCH_3	H		3,4-OCH_2O-	0,672
6	Allyl	OCH_3	OCH_3	H	H	4-Br	0,724
7	Allyl	OCH_3	OCH_3	H	H	4-NO_2	1,097
8	Allyl	O-Allyl	OCH_3	H	H	4-Cl	0,892
9	H	O-Allyl	OCH_3	H	H	4-Cl	0,398
10	H	O-Allyl	OCH_3	H	3-Cl	4-Cl	1,000
11	H	O-Allyl	OCH_3	H	H	4-Br	0,908
12	H	O-Allyl	OCH_3	H	H	4-F	1,362
13	H	O-Allyl	OCH_3	H	H	3-Cl	0,724
14	H	O-Allyl	OCH_3	H	H	4-OCH_3	1,352
15	H	O-Allyl	OCH_3	H		3,4-O-CH_2-O-	1,585
16	H	O-Allyl	OCH_3	H	H	4-NH_2	1,556
17	H	O-Allyl	OCH_3	H	H	H	1,580
18	H	OH	OCH_3	H	H	4-Cl	1,447
19	H	O-Prényl	OCH_3	H	H	4-Cl	0,699
20	H	O-Butyl	OCH_3	H	H	4-Cl	1,170
21	OCH_3	O-Allyl	OCH_3	H	H	4-Cl	0,580
22	H	O-Allyl	H	H	H	4-Cl	1,633
23	H	H	H	O-Allyl	H	4-Cl	0,954
24	H	Cl	H	H	3-O-Allyl	4-OCH_3	0.934

2.2 Model, calculations and applications

The Gaussian03 package of software [40] was used to optimize the geometry of all molecules in their neutral form. The calculations were performed within the Density Functional Theory (DFT) at the B3LYP/6-31G(d,p) level. The D-Cent-QSAR software [41] was used to calculated the local atomic reactivity indices from the single point results of Gaussian03. All electron populations lesser than or equal to 0.01e are considered null [42]. The orientational parameters of the substituents are calculated in the usual manner [43-44]. We used the concept of common skeleton defined as a set of atoms common to all the molecules analyzed. We hypothesize that the variation of the numerical values of the local atomic reactivity indices (LARIs) of the atoms of this common skeleton accounts for almost all the variation of the biological activity. The numbering of the atoms of the common is shown in Fig. 2.

As the number of LARIs involved is greater that the number of molecules, the solving of the linear systems of equations is not possible. For this reason we employed the technique of linear multiple regression analysis (LMRA) to determine the atoms that are directly involved in the variation of the biological activity. The data matrix contains

log (IC_{50}) as a dependent variable, and the local atomic reactivity indices of all the atoms of the common skeleton as independent variables. The Statistica software was used to perform LMRA studies [45].

3. Results

The best statistically significant equation obtained is:

$$\log(IC_{50}) = 8.17 + 1.63\mu_9 - 0.04S_8^N(LUMO+2)^* + 0.86F_{11}(HOMO-1)^* + 1.03F_{12}(LUMO+1)^*$$
$$0.003S_{12}^N(LUMO+1)^* - 0.66F_{14}(HOMO-2)^* - 2.03F_5(HOMO-1)^* + 0.49Q_{13}$$

With statistical parameters (n = 24, (R = 0.99, R^2 = 0.98, R^2adj = 0.97, F (8.15) = 94.89, (p-Value <0.000001), a standard error estimated at 0.14 and absence of outliers outside the ± 2σ limit.) The following indices of reactivity have been grouped into four different types:

μ_9 is the local atomic electronic chemical potential of atom 9,

$S_8^N(LUMO+2)^*$ is the atomic nucleophilicsuperdelocalizability of third lowest vacant MO on atom 8;

$F_{11}(HOMO-1)^*$ is the Fukui index of the second highest occupied MO located on atom 11;

$F_{12}(LUMO+1)^*$ is the Fukui index of the second lowest vacant MO located on atom 12;

$S_{12}^N(LUMO+1)^*$ is the atomic nucleophilicsuperdelocalizability of second lowest vacant MO on atom 12;

$F_{14}(HOMO-2)^*$ is the Fukui index of the third highest occupied MO located on atom 14;

$F_5(HOMO-1)^*$ is the Fukui index of the second highest occupied MO located on atom 5;

Q_{13} is the charge of atom 13.

The values of the beta coefficients, the t-tests (Tab II) obtained are very significant for the variables of equation (2). The highest internal correlation value is 0.41 (TabIII), is observed between the independent variables $S_{12}^N(LUMO+1)^*$ and $F_{12}(LUMO+1)^*$. Figure 3 shows the curve showing a good relationship between the log (IC_{50}) values observed and those calculated. Table IV shows the Local Molecular Orbitals of atom 5, 8, 11, 12 and 14 (see Fig. 3). Nomenclature: Molecule (HOMO) / (HOMO-2)* (HOMO-1)* (HOMO)* - (LUMO)* (LUMO+1)* (LUMO+2)*. The number corresponding of the HOMO of each molecule is in bracket, and for each atom we have the third local HOMO* and the third local LUMO*.

The statistical parameters associated with equation (2) show that this equation is statistically significant and involves the variation of eight local indices of atomic reactivity along the skeleton common to 97% of the log variation (IC_{50}).

Table II: Beta coefficients and t-test for significance of coefficients in Eq. 2.

Variable	Beta coefficients	t(15)	p-Value
μ_9	0.99	21.09	0.000000
$S_8^N(LUMO+2)^*$	-0.57	-14.05	0.000000
$F_{11}(HOMO-1)^*$	0.27	6.96	0.000005
$F_{12}(LUMO+1)^*$	0.53	9.34	0.000000
$S_{12}^N(LUMO+1)^*$	0.46	7.75	0.000001
$F_{14}(HOMO-2)^*$	-0.40	-8.72	0.000000
$F_5(HOMO-1)^*$	-0.30	-6.42	0.000012
Q_{13}	0.25	4.17	0.000817

Table III: Coefficient of correlation between variables appearing in Eq.2

	μ_9	$S_8^N(LUMO+2)*$	$F_{11}(HOMO-1)*$	$F_{12}(LUMO+1)*$	$S_{12}^N(LUMO+1)*$	$F_{14}(HOMO-2)*$	$F_5(HOMO-1)*$
$S_8^N(LUMO+2)*$	0.06						
$F_{11}(HOMO-1)*$	0.01	0.0001					
$F_{12}(LUMO+1)*$	0.0001	0.002	0.04				
$S_{12}^N(LUMO+1)*$	0.16	0.006	0.02	0.41			
$F_{14}(HOMO-2)*$	0.07	0.06	0.08	0.001	0.002		
$F_5(HOMO-1)*$	0.04	0.002	0.02	0.11	0.25	0.08	
Q_{13}	0.15	0.07	0.06	0.37	0.35	0.06	0.18

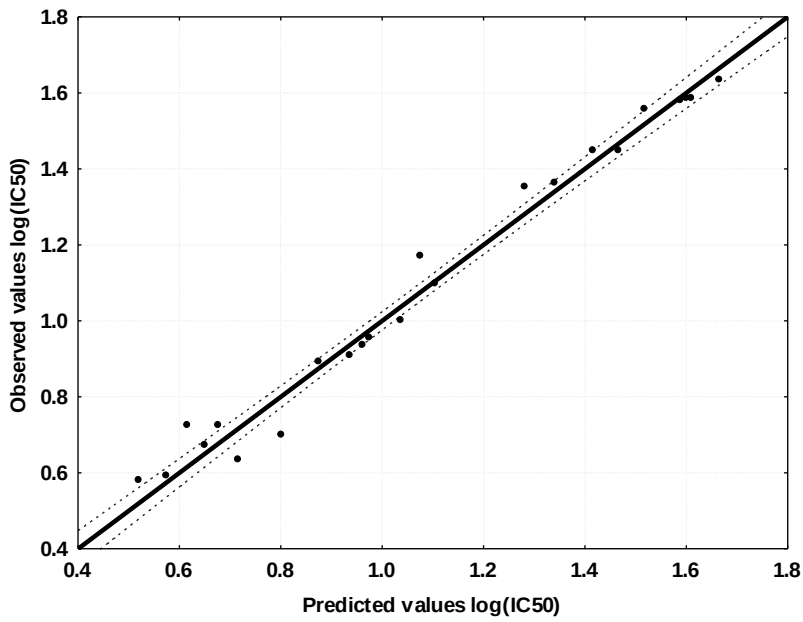

Figure 3: Plot of predicted vs. observed log(IC_{50}) values. Dashed lines denote the 95% confidence interval

Table IV: Local Molecular Orbitals of atom 5,8,11,12 and 14

Molecule (HOMO)	Atom 5 (C)	Atom 8 (C)	Atom 11 (C)	Atom12 (C)	Atom14 (C)
1(82)	75π76π82π-83π84π85π	79π80π82π-83π84π85π	77π80π81π-83π84π85π	77π80π81π-84π85π86π	77π81π82π-84π85π88π
2(86)	78π80π86π-87π88π89π	84π85π86π-87π88π89π	81π83π84π-87π88π89π	81π83π84π-87π88π89π	81π83π84π-88π89π91π
3(90)	83π89π90π-91π92π93π	88π89π90π-91π92π93π	85π87π88π-91π92π93π	85π87π88π-91π92π93π	85π87π88π-92π93π95π
4(90)	84π88π90π-91π92π94π	87π88π90π-91π92π94π	85π87π89π-91π92π93π	85π87π89π-93π94π96π	85π89π90π-92π93π96π
5(93)	91π92π93π-94π95π96π	91π92π93π-94π95π97π	88π90π92π-94π95π96π	90π92π93π-95π96π97π	88π92π93π-95π96π97π
6(99)	92π98π99π-	97π98π99π-	94π96π97π-	94π96π97π-	94π96π97π-

	100π101π102π	100π101π102π	100π101π102π	100π101π102π	101π102π104π
7(93)	85π92π93π-95π97π98π	91π92π93π-94π95π97π	88π89π90π-94π96π97π	88π89π90π-94π95π96π	87π88π89π-94π95π96π
8(97)	89π96π97π-98π99π100π	95π96π97-98π99π100π	93π94π95π-98π99π100π	93π94π95π-98π99π100π	93π94π95π-99π100π103π
9(86)	80π85π86π-87π88π89π	84π85π86π-87π88π89π	81π83π84π-87π88π89π	81π83π84π-87π88π89π	81π83π84π-88π89π92π
10(94)	87π93π94π-95π96π97π	92π93π94π-95π96π97π	89π91π92π-95π96π97π	89π91π92π-95π97π99π	85π86π89π-96π97π99π
11(95)	89π94π95π-96π97π98π	93π94π95π-96π97π98π	90π92π93π-96π97π98π	90π92π93π-96π97π98π	92π93π94π-97π98π100π
12(82)	76π81π82π-83π84π85π	80π81π82π-83π84π85π	77π79π80π-83π84π85π	77π79π80-84ππ85π88π	77π79π80π-84π85π88π
13(86)	79π85π86π-87π88π89π	84π85π86π-87π88π89π	81π83π84π-87π88π89π	78π83π84π-87π88π89π	81π83π84π-88π89π92π
14(86)	80π83π86π-87π88π89π	83π84π86π-87π88π92π	82π84π85π-87π88π89π	82π84π85π-88π89π92π	82π85π86π-88π89π92π
15(89)	87π88π89π-90π91π92π	87π88π89π-90π91π92π	86π88π89π-90π91π92π	85π88π89π-91π92π93π	81π85π89π-91π92π93π
16(82)	79π81π82π-83π84π85π	80π81π82π-83π84π87π	78π80π82π-83π84π85π	80π81π82π-85π86π88π	78π81π82π-84π85π88π
17(78)	72π76π78π-79π80π81π	76π77π78π-79π80π84π	69π74π77π-79π80π81π	74π75π77π-79π80π81π	69π74π75π-80π81π84π
18(75)	70π73π75π-76π77π78π	73π74π75π-76π77π78π	71π72π74π-76π77π78π	71π72π74π-76π77π78π	71π72π73π-77π78π80π
19(94)	88π92π94π-95π96π97π	92π93π94π-95π96π97π	89π91π93π-95π96π97π	91π92π93π-95π96π97π	89π91π92π-96π97π100π
20(91)	86π89π91π-92π93π94π	89π90π91π-92π93π94π	88π89π90π-92π93π94π	88π89π90π-92π93π94π	88π89π90π-93π94π96π
21(94)	84π85π94π-95π96π97π	91π92π94π-95π96π97π	89π91π92π-95π96π97π	89π91π92π-95π96π97π	89π91π92π-96π97π100π
22(78)	70π72π78π-79π80π82π	76π77π78π-79π80π82π	75π76π77π-79π80π81π	75π76π77π-79π80π81π	75π76π77π-80π81π84π
23(78)	72π76π78π-79π80π81π	76π77π78π-79π80π83π	75π76π77π-79π80π81π	75π76π77π-79π80π81π	74π75π76π-80π81π84π
24(86)	79π85π86π-87π88π89π	84π85π86π-87π88π89π	84π85π86π-87π88π89π	84π85π86π-88π90π91π	82π83π86π-88π89π90π

4. Discussion

The results obtained indicate that a good antiplasmodial activity of these 24 chalcone derivatives is related to the variation of the different numerical values of all eight local indices of atomic reactivity along the common skeleton. This result is very good considering the approximations made to build the model.

From the comparison of the values of the beta coefficients it follows the importance in descending order of the following variables: $F_5(HOMO-1)^* > \mu_9 > F_{12}(LUMO+1)^* >$
$F_{11}(HOMO-1)^* > F_{14}(HOMO-2)^* > Q_{13} > S_8^N(LUMO+2)^* > S_{12}^N(LUMO+1)^*$

The process seems to be orbital and charge-controlled because the indices on the electron population or/and the energies of MOs and the charge.

Variable by Variable Analysis indicates that a good antiplasmodial activity is associated with the high negative value of μ_9, the high positive value of $S_8^N(LUMO+2)*$, $F_{14}(HOMO-2)*$, $F_5(HOMO-1)*$, the low positive value of $F_{11}(HOMO-1)*$, $F_{12}(LUMO+1)*$, $S_{12}^N(LUMO+1)*$ and the high negative value of Q_{13}. All the orbitals implicated on the process are π nature (Tab IV).

Atom 9 is a carbon atom of the carbonyl group, the high negative value of μ_9 indicates that atom 9 act as an electroacceptor site that must interact with an electron rich center of the receptor.

Atom 8 is a carbon atom, the high positive value of $S_8^N(LUMO+2)*$ should be obtained whether by raising the Fukui index on $(LUMO+2)_{15}*$ or by lowering the $(LUMO+2)_{15}*$ energy. In the two cases, the three lowest LUMO should be more reactive. So atom 8 interacts with an electron rich center through its π empty orbitals.

Atom 11 is a carbon atom of the phenyl that links to the carbonyl group. The presence of $(HOMO-1)_{11}*$ implies that $(HOMO)_{11}*$ participates to the process. The low positive value of $F_{11}(HOMO-1)*$ indicates that atom 11 interacts with an electron rich center through its highest occupied orbitals. This interaction could be π-π, or π-σ kind.

Atom 12 is a carbon atom of the phenyl that links to the carbonyl group. The low positive value of $F_{12}(LUMO+1)*$ indicates that atom 12 interacts with an electron-deficient center such as a cation. This is in perfect agreement with the low value of $S_{12}^N(LUMO+1)*$.

Atom 14 is a carbon atom of the phenyl that links to the carbonyl group. The low positive value of $F_{14}(HOMO-2)*$ indicates that atom 14 interacts with an electron rich center.

Atom 5 is a carbon of one phenyl ring. The high positive value of $F_5(HOMO-1)*$ indicate that atom 5 should interacts with an electron-deficient center.

Atom 13 is a carbon atom of the phenyl that links to the carbonyl group. The positive sign of the coefficient of the net charge Q_{13} imposes us the choice of a high negative value of this index on the carbon atom 13 and induces the necessity that it interacts with a positive site.

All these suggestions are presented in the partial 2D inhibition pharmacophore on Figure 5.

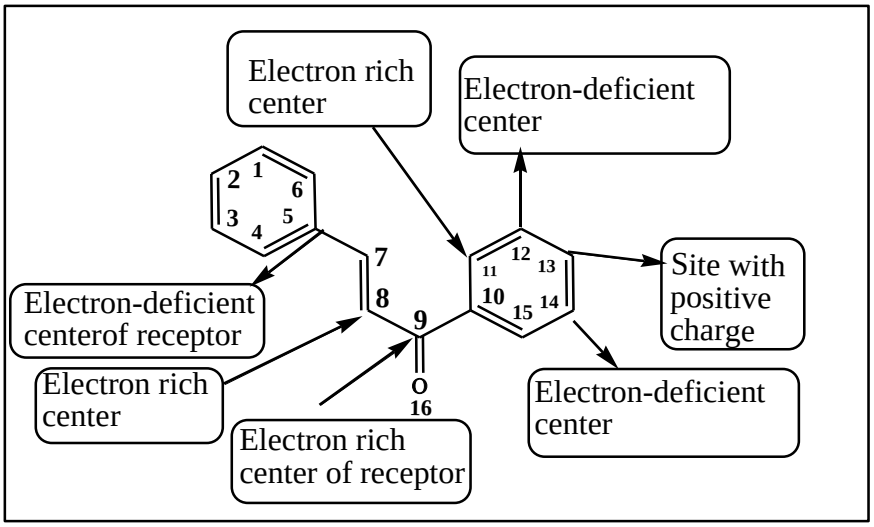

Figure 4: Partial 2D-Pharmacore for antiplasmodial activity of chalcone derivatives on plasmodium falciparum strain pf3D7

4. Conclusion

We obtained a statistically significant relationship between the variation of the antiplasmodial activities of some chalcone derivatives and the variation of the numerical values of a set of local atomic reactivity indices. We propose a model of 2D-pharmacophore. It follows that the choice, the nature, and the position of a substitute to be grafted on the electronic structure of the skeleton are decisive for obtaining good antipasmodial activity. Thus the regression equation obtained could serve as a tool for predicting the antiplasmodial activity of other chalcones.

Acknowledgments

We thank Juan S. Gomez-Jeria, who accept to perform one part of the calculation on the computers of the Quantum PharmacologyUnit of the University of Chile.

References

1. Aubry, P., & Gaüzère, B. (2017). Centre René Labusquière, *Institut de Médecine Tropicale, Université de Bordeaux*, 33076 Bordeaux (France).
2. Nicholas, E., & Ashley, A. (2014). The duration of Plasmodium falciparum infections, *White Malaria Journal*.13:500
3. M. Mishra, V.K. Mishra, V. Kashaw, A.K. Iyer, S.K. Kashaw, (2017), Comprehensive review on various strategies for antimalarial drug discovery, *Eur. J. Med. Chem.*, 125 1300–1320.
4. Portet, B., (2007) Bioguidee search for antimalarial molecules of a Guyanese plant Piper hostmannianum var. berbicense. *Thesis University Toulouse III - Paul Sabatier*. 10-19.
5. Traore, M., (2012). Microbiology and Parasitology, University of the Grenoble Alps.
6. Chavain, N., (2008). Conception, synthèse, analyse strucurale et activité antipaludique de dérivés de la ferroquine. Chimie Organique et Macromoléculaire, *Thèse de doctorat.University. Lile*.
7. Kien, & Kremer M., (1980). *CAHIERS O.R.S.T.O.M*. vol. XVIII - NO2 -. Paris :s.n., pp. 147-186.
8. Epaulard, O. (2016). *Department of Infectious Diseases Therapeutics anti-infectious CHU of Grenoble*.
9. Organization, (2012). World Health. *Geneva, Switzerland*, January 2016.
10. Wilson A. L., (2011). Taskforce IP .*PLoS One.* ; 6 (2): e16976.
11. Meremikwu, M. M. al. (2012). *Cochrane Database Syst Rev.* (2): CD003756.
12. Organization. (2016) World Health. *Geneva, Switzerland*, 2012.
13. Moorthy, V. S., Ballou, W., & Malar, I. (2009). Journal 2009.
14. Organization (WHO) (2015). *World Health*, 2015.
15. Leach, A., & al. (2011). *Clinical trials Partnership. s.l.*: Malar January. 2011.
16. Siddiqui, Z. N., & al. (2012) *J. Enz. Inhib. Med. Chem.*, 27, 2012, 84-91.
17. Seo, W., Ryu, Y., Curtis-Long, M., Lee, C., Ryu, H., & Jang, K., (2010). *Eur. J. Med.Chem.*, 45, 2010, 2010-2017.
18. Trivedi, J. C., Bariwal, J. B, Upadhyay K.D, Naliapara, E. D Joshi, S. K, (2007). Pannecouque, C. C., Clercq, E. D., & Shah, A. K. (2007). *Tetrahedron Lett.*, 48, 8472-8474.
19. Bonesi., M., Loizzo, M. R., Statti, G. A., Michel, S., Tillequin, F., &Menichini, F., (2010). *Bioorg. Med. Chem. Lett.*, 20, 1990-1993.
20. Li, R., Chen, X., Gong, B., Dominguez, J. N., Davidson, E., Kurzban, G., Miller, R. E, Nuzum, E. O., Rosenthal, P. J., & McKerrow, J. H. (1995). *J. Med. Chem.*, 38, 5031–5037.
21. Kumar, R., Mohanakrishnan, D., Sharma, A., Kaushik, N. K., Kalia, K., Sinha , A. K., & Sahal, D. (2010). *Eur. J. Med. Chem*., 45, 5292–5301.
22. Hans, R. H., Guantai, E. M., Lategan, C., Smith, P. J., Wan, B., Franzblau, S. G., Gut, J., Rosenthal, P. J. , & Chibale, K. (2010). *Bioorg. Med. Chem. Lett.*, 20, 2010, 942–944.
23. Sharma, N., Mohanakrishnan, D., Shard, A., Sharma, U. K., Kumar, R., Richa, Sinha, A. K., & Sahal, D. (2014). *Eur. J. Med. Chem*., 79, 350-368.

24. Sashidhara, K. V., Avula, S. R., Palnati, G. R., Singh, S. V., Srivastava, R. K., Puri, S. K., Saxena J. K. (2012). *Bioorg. Med. Chem. Lett.*, 22, 5455–5459.
25. Karelson, M., Lobanov, V., S., & Katritzky, A. R., (1996). *Chem. Rev*., 96, 1027–1044.
26. Tadigoppula, N., Korthikunta, V., Gupta, S., Kancharla, P., Khaliq, T., Soni, A., Srivastava, R., K., Srivastava, K., Puri, S., K., Raju, K. S. R., WahajuddinSijwali, P. S., Kumar, V., & Mohammad, I. S. (2013). *J. Med. Chem.*, 56, 31−45.
27. Gómez-Jeria, J. S. (2013) A New Set of Local Reactivity Indices within the Hartree-Fock-Roothaan and Density Functional Theory Frameworks. *Canad. Chem. Trans.* 1, 25-55.
28. Gómez-Jeria, J. S. & Ojeda-Vergara, M. (2003) *J. Chil. Chem. Soc.* 48.
29. Gómez-Jeria, J. S. & Maruani, J. (1989). *Ed., Springer Netherlands*, pp. vol. 4, pp. 215-231.
30. Gómez-Jeria, J. S. (1983) *Int. J. Quant. Chem.*, 23.
31. Fukui, K., & Fujimoto, H., (1997) *World Scientific: Singapore; River Edge, N.J*.
32. Gómez-Jeria, J. S. & Ojeda-Vergara, M. (2003) *J. Chil. Chem. Soc.*, 48.
33. Leal, M. S., Robles-Navarro, A. & Gómez-Jeria, J. S. (2015). *Der Pharm. Lett.*, 7.
34. Gómez-Jeria, J. S. & Robles-Navarro, A. (2015). *Res. J. Pharmac. Biol. Chem. Sci*., 6.
35. Gómez-Jeria, J. S. & Valdebenito-Gamboa, J. A. (2015*). Der Pharm. Lett.*, 7.
36. Gómez-Jeria, J. S. & Robles-Navarro, A. (2015). *J. Comput. Methods Drug Des.*, 5.
37. Gómez-Jeria, J. S. & Robles-Navarro, A. (2015). *Res. J. Pharmac. Biol. Chem*. Sci., 6.
38. Gómez-Jeria, J. S. & Robles-Navarro, A. (2015). *Der Pharma Chem.*, 7.
39. Nandini, S., Dinesh, M., Upendra, K., S., Rajesh, K., Richa, A., Kumar, S., & Dinkar, S. (2014). *European Journal of Medical Chemistry*.
40. Frisch, M. J., Trucks, G. W., Schlegel, H. B., Scuseria, G. E., Robb, M. A., Cheeseman, J. R., Montgomery, J., J.A., Vreven, T., Kudin, K. N., Burant, J. C., Millam, J. M., Iyengar, S. S., Tomasi, J., Barone, V., Mennucci, B., &Cossi, M. (2007) Scalmani, G03 *Rev. E.01, Pittsburgh*, PA, USA.
41. Gómez-Jeria, J. S. *D-Cent-QSAR: A Program to Generate Local Atomic Reactivity Indices from Gaussian 03 Log Files. 1.0*, Santiago, Chile. 2014
42. Gómez-Jeria, J. S. (2009) *J. Chil. Chem. Soc*., 54.
43. Gómez-Jeria, J.S. (2016). *Research Journal of Pharmaceutical, Biological and Chemical Sciences*, 7, 288-294.
44. Gómez-Jeria, J. S. (2016). *Research Journal of Pharmaceutical, Biological and Chemical Sciences*, 2016, 7, 2258-2260.
45. Statsoft, Statistica 8.0, (2300). *East 14th St*. Tulsa, OK 74104, USA 1984-2007.